Article:

Sunar, Ö and Fletcher, D. (2023) Experimental investigation on the arc damage and fatigue crack initiation risk of copper-silver contact wires. IEEE Transactions on Power Delivery, 38 (2). pp. 777-784. ISSN: 0885-8977

https://doi.org/10.1109/tpwrd.2022.3198734

Experimental Investigation on the Arc Damage and Fatigue Crack Initiation Risk of Copper-Silver Contact Wires

Özgün Sunar, David Fletcher

Abstract

Contact wires are subjected to both mechanical and electrical interactions while electrical energy is transmitted to the trains by overhead lines and train pantographs. Particularly, an increase in the speed of trains can result in greater contact force fluctuations and more intense pantograph arcs, therefore, these mechanical and electrical interactions have potential to drive failure of Overhead Line Equipment (OLE) conductors. In this paper, the effect on fatigue crack initiation risk of material ablation from the contact wire surface due to arc discharge is experimentally investigated under laboratory conditions. Fatigue life, crack propagation directions and crack initiation locations in arc-exposed copper silver contact wire samples are compared with those in comparable arc-free samples. The results show that having arc damage on the contact wire surface could result in 50% shorter fatigue life compared to arc-free contact wires. It is often considered that wear rather than fatigue cracking defines the life of the contact wires, but under some conditions with the combination of arcing, the fatigue life in the contact wire can become the controlling failure risk. Therefore, in determining system life and maintenance requirements the fatigue life of the contact wire should be taken into consideration at locations where the arc discharge is likely.

Keywords

Fatigue, arc damage, contact wire, Overhead Line Equipment

1. Introduction

Overhead line equipment (OLE) is used for transmitting electrical energy to trains in railway electrification. This transmission occurs with physical and electrical contact of the pantograph and contact wire pair. Contact wires, usually copper alloy materials [1], are supported by messenger wires, OLE fittings and OLE structures to provide a steady current collection quality for the pantograph. To maintain contact and increase the current collection quality, the pantograph also applies an uplift/contact force to the contact wire (Figure *1*)

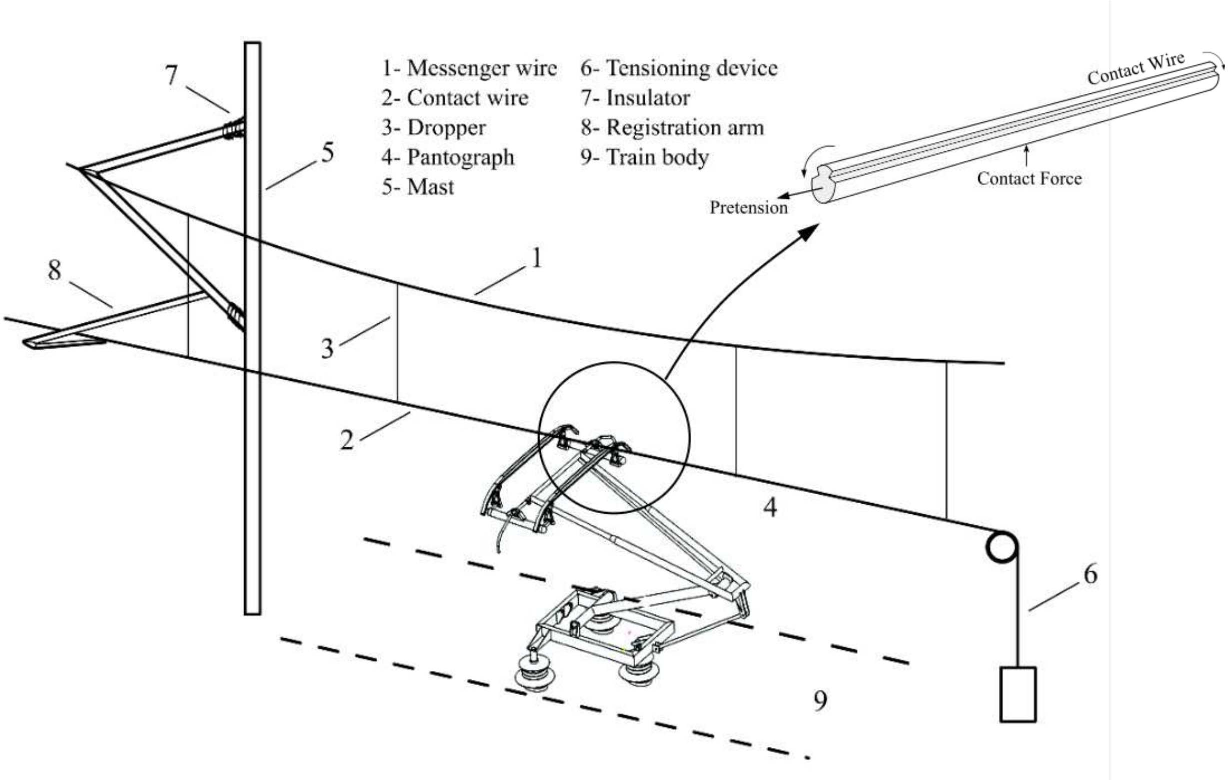

Figure 1 Schematic of OLE components

For many years, considering contact force applied to the sliding pantograph-wire interface the wear life of the contact wire was considered one of the most important criteria in determining the design life of OLE systems. However, recent studies showed that fatigue can be the life limiting factor and the contact wire can fail or require replacement prior to its expected wear life [2]–[5]. Kim et al. [6] explained the main reason for the contact wire fatigue by considering the bending strain due to the contact force.

In the literature, experimental methods dominate in research determining the fatigue behaviours of OLE contact wires. Several fatigue test configurations exist with the most common using 2-3 metres length of tensioned contact wire and a single point contact in the centre of the specimen [7], [8]. The main difference between the designs is the mechanism triggering the vertical oscillation. Some designs use a crack-motor mechanism to oscillate the contact wire sample while others used linear servo motor or hydraulic actuator [9], [10]. However, Sunar et al. [11] proposed a new experimental configuration which accommodated a 400mm-length contact wire using a combination of bending and pretension to replicate service conditions found in longer spans. The much shorter length of wire used was an advantage for comparative tests focused on novel wire metallurgy for which only limited supplies existed, and in study of cracks propagating from known sites of surface damage.

Besides contact load variation additional studies have showed that there are other factors accelerating the fatigue failures in OLE contact wire. Firstly, Nguyen et al. [12] observed fatigue crack failures near junction claws during visual inspections in track. In this type of fatigue a crack propagated from bottom to the top of the contact wire. In the same vein, Network Rail [13] reported a similar crack behaviour which occurred near a junction claw just after two years from installation. The high stiffness and heavy weight of the OLE fittings relative to the contact wire were found to be the main reason for these rapid fatigue fractures. The second factor identified as affecting the fatigue life is pretension in the OLE contact wire. From a design perspective the pretension is used for preventing sagging in the line and also controls the speed of wave propagation along the line affecting pantograph contact stability. However, this pretension generates a mean stress in the contact wire and if not corrected the mean stress becomes larger with the decrease in the contact wire section due to the wear. Yamashita et al. [7] showed that when the wear reached up to 40% of the original cross-section fatigue life of the contact wire could drop to one third of that originally expected. Therefore, the wear, as a result of increased mean stress, increases the vulnerability of the contact wire to the fatigue even when the passage of pantographs and their contact force applies only small amplitude forces.

The effect of arcs on contact wire life has received little attention in published literature. Li et al. [14], [15] found that sparks and electric arc formation between contact wire and the pantograph strip could lead to poorer mechanical performance of the contact wire material. This was the result of the rapid heating and cooling of a small volume of material local to the arc contact point on the overhead wire. Massat et al. [16] identified surface defects on the contact wire due to the pantograph friction and electrical arcs and mentioned that these surface defects could increase the risk of fatigue crack initiation. Sunar et al. [17] conducted a systematic experimental study about quantifying the arc damage to the contact wire and found that microcracks and voids occurred beneath the contact wire surface after single or repeating arc(s). Their analysis of contact wire withdrawn from service identified that arc damage could take place on any surface of the contact wire (bottom, top or sides) as results of pantograph or flashover arcs. Moreover, microcracks and voids were identified at sites of arc events that could play a significant role in fatigue crack initiation [18].

The studies presented thus far provide evidence that there are multiple factors influencing the fatigue life of contact wire, particularly in the cases where the rapid fatigue failures occurred long before the expected service life. Several studies have identified that the mean stress (additional tension) and OLE fittings (dynamic load due to change of stiffness) are substantial in determining the fatigue life of the contact wire. However, the aspects of whether arc related surface damage plays an important role in determining the fatigue life of the contact wire is relatively unexplored. This study therefore sets out to extend understanding of whether surface damage caused by arcing can trigger fatigue crack initiation and affect the fatigue life behaviours of the contact wire.

2. **Methods**

In order to identify the effect of surface arcs on fatigue life of contact wires two experimental configurations were used. Firstly, contact wire samples were subjected to arcs in the SOLARC machine (see Section 2.2) which replicates the pantograph to contact wire arc in a controlled lab environment. Secondly, arc-affected contact wire samples were loaded cyclically on a hydraulic fatigue test machine equipped with an OLE fatigue fixture (see Section 2.4) enabling the fatigue life results of arc affected contact wire samples to be compared with those of arc-free contact wire. The methodology is shown schematically in Figure 2.

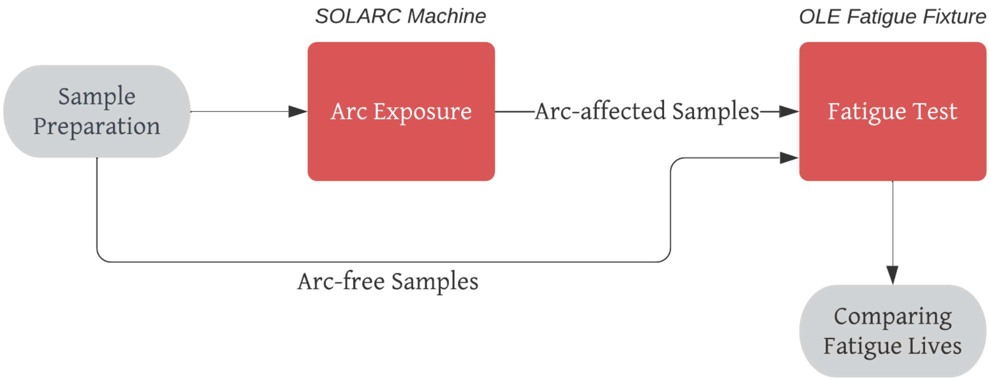

Figure 2 Flow chart of the methods used in assessing effects of arcing on fatigue life of OLE contact wires

2.1. Sample Preparation

Copper-silver contact wire type AC120 was prepared as 400 mm samples for use in the experiments. The wire was a commercially supplied grade compliant with standard EN 50149 [1]. The standard shows that the electrical resistance of copper-silver OLE contact wire with a nominal content of 0.1 % Ag and 0.04 % oxygen by weight [1] is 0.122 Ω/km. Its hardness was confirmed experimentally to be in the range 115-122 HV in a separate strand of the research [17].

The wires were commercially supplied in new undamaged condition (free of the oxide layer or wear) as would be used for installation. The specimen preparation process was carried out so as to avoid introducing any imperfection (roughness, inclusion and cracks) that would be expected to affect fatigue failure initiation. This differs from many conventional fatigue tests in which a highly polished specimen would be required. Here the 'as installed' condition of real OLE wire as a component was of interest rather than an abstract material study. In addition to observation of crack faces at the termination of fatigue testing additional samples were prepared for metallographic observation to reveal the arc damage in the material's interior (and comparable none arc exposed material) prior to the application of fatigue stress cycles.

2.2. SOLARC Machine

Sheffield Overhead Line Arc Machine (SOLARC) [17] was used for creating arc-affected contact wire samples. The SOLARC machine's active components are a linear solenoid, pantograph contact strip sample, contact wire sample and a power supply. SOLARC can be set up to generate arcs with both direct and alternating current, however, in this study only DC arcs were created. Contact and break motions of the carbon strip sample were driven by the linear solenoid with duration, interval time and the number of arcs controlled by a programmable microcontroller to ensure repeatability. This controller conducted the actuation of a linear solenoid driving motion of the contact strip sample. A high-speed camera system (Basler Sprint spl4096-70kc with Nikon Al-s 105mm f/2.8 macro lens) was used for determining the position and the movement of the contact strip sample during the experiments. Figure *3* shows SOLARC machine configuration.

Voltage dividers and current probes (Pico TA019) were used for detecting arc current, voltage and duration, connected to the electrical circuit as shown in Figure *3*a. Processing of the signals from the current probe and voltmeter was established by a digital oscilloscope (Picoscope model 2000 series) with logging of data to a computer.

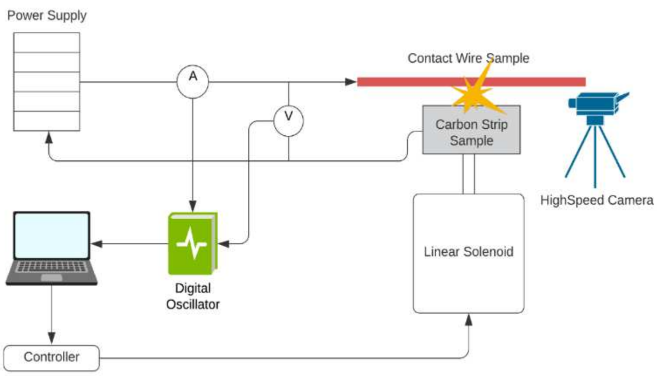

a) Schematic of experimental setup

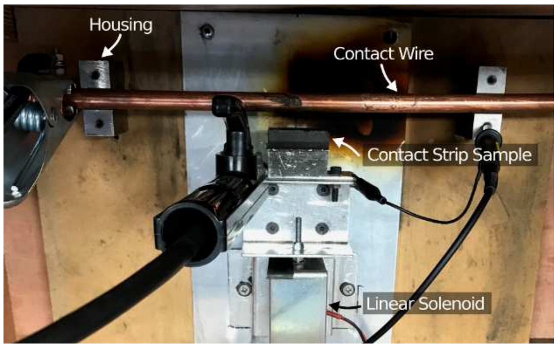

b) Internal picture of enclosed SOLARC machine

Figure 3 SOLARC machine test configuration

The SOLARC machine was built in an environmental enclosure with interlocking switches to prevent access during the experiments. The enclosure was equipped with an extractor fan to remove any smoke or fumes generated. Sliding interaction between pantograph carbon and contact wire was not present in the tests which aimed to gain understanding of the electrical aspects of the contact prior to future combined mechanical and electrical testing. Contact wire samples were in a straight form, thus additional tensioning force was not applied during the arc tests.

2.3. Arc Exposure

The arc exposure stage was completed with 20 different samples for 200 A DC current. The DC power supply was selected because DC OLE systems typically suffer longer duration and consequently higher energy arc events. This is because the unidirectional current does not present the zero crossing point of an AC power cycle that tends to break an existing arc. The amount of energy released due to the arc discharge is therefore greater than that of AC, and more severe surface damage is expected.

Arcs were generated between the pantograph contact strip sample and the contact wire as a consequence of the motion of the linear solenoid. shows change in voltage and current based on the position of the contact strip sample. Initially, at the time of zero, the contact strip sample and the contact wire was apart. Stage I, Stage II and Stage III, indicated the approaching arc, full contact and drawing arc stages, respectively. Duration of arcs (approaching and drawing) was detected to be 300 ms ± 10 ms. Although this experimental configuration was equipped with a power supply which had a typical DC characteristics, steady and unidirectional open circuit voltage, in Stage 3 when the mechanical contact broke between the contact wire and the contact strip sample, the electrical contact was sustained a certain time throughout the arcs and this resulted in fluctuations in voltage and current until the gap reached a level that broke the arc between the two materials (contact wire sample and carbon strip sample). The energy input quantified through voltage and current measurements was just below 1.40 kJ.

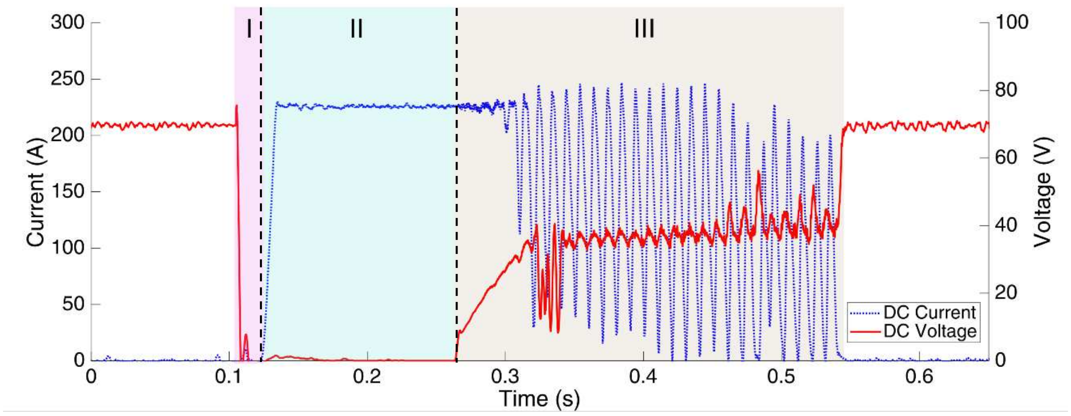

a) *Voltage and current variation during a single arc. The current remains uni-directional although undergoes rapid fluctuations during the period of arcing as the power supply responds to the arcing process.*

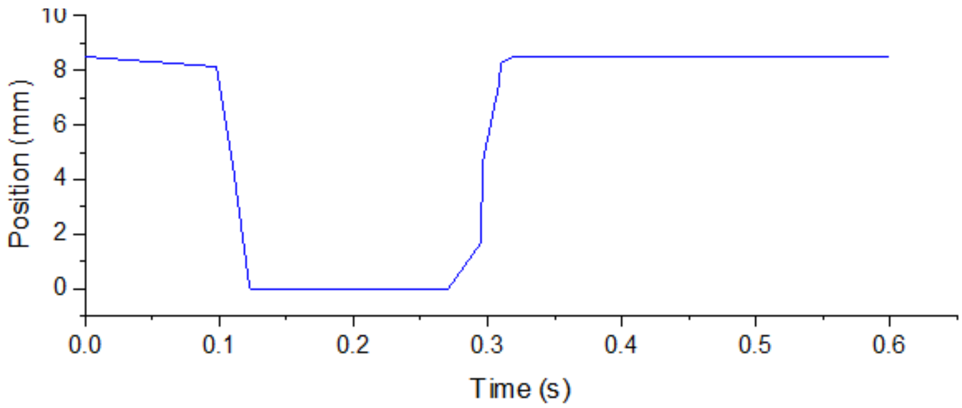

b) *The gap between carbon strip sample and contact sample over time*

Figure 4 Voltage and current characteristics of a single arc with position variation of carbon strip sample during arcing process

2.4. OLE Fatigue Apparatus

Fatigue testing was conducted using 400-mm-length contact wire samples according to ASTM [19] four-point bending principle, modified with the addition of axial tension. An existing OLE fatigue test bench (Figure 5a, [11]) developed at The University of Sheffield was used to conduct the study. In this machine, the working section between the left support and right support subject to bending was 300 mm. Axial tension and lateral constraint was achieved using OLE connection clamps available commercially to suit the wire being tested.

The arc affected location on the contact wire may differ slightly between tests because of the nature of arc formation at the interface with the pantograph carbon in the SOLAR machine. It is therefore important that the fatigue test outcome is insensitive to the exact location of this damage within the samples. One of the main advantages of using four-point bending is that it provides a uniform moment distribution free of shear stress throughout the 300mm working section. Arc induced pre-damage simply needs to lie within this region (preferably away from the points of load application) for it to be subject to well quantified uniform bending. The contact wire samples can be accommodated with the arc affected side in either an upper or lower position in this apparatus (Figure 5b) changing the stress experienced at the damage location. Although the contact wire sample was required to be 'upside down' relative to real-world installation due to hydraulic actuator's location, in all cases the bottom and top locations of contact wire samples were referred by their in-service orientations.

Beside the four-point bending, the contact wire was held under pretension to replicate realistic working conditions with both bending and tensioning acting together. Contact wire tensioning was applied using the lever arm (Figure 5c). The contact wire sample is held by two rotational bearings giving rotational freedom at the support points. One bearing is fixed in the sample longitudinal direction while a pillow type bearing was selected to allow linear motion at the other bearing thereby enabling tensioning (this type or bearing has sufficient endurance life for long term fatigue tests). A weight applied the pretension to the contact wire at the far-left end of the apparatus. The tensioning arm provided a 1:10 force ratio.

Vertical bending was driven by a sine wave motion at 5 Hz in the current tests, although more complex load-time histories from field data or modelling predictions could also be applied using the same equipment. The vertical load was measured by using a load cell with 5kN capacity (RLT0500, RDP

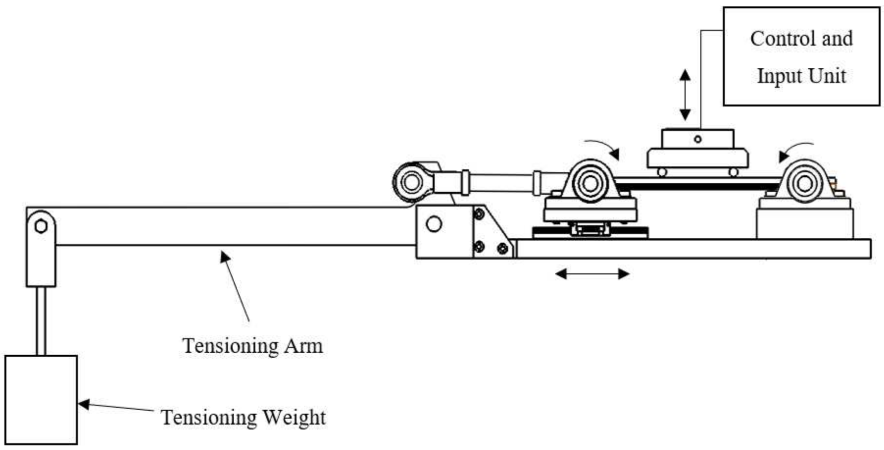

a) Working principles of OLE fatigue apparatus

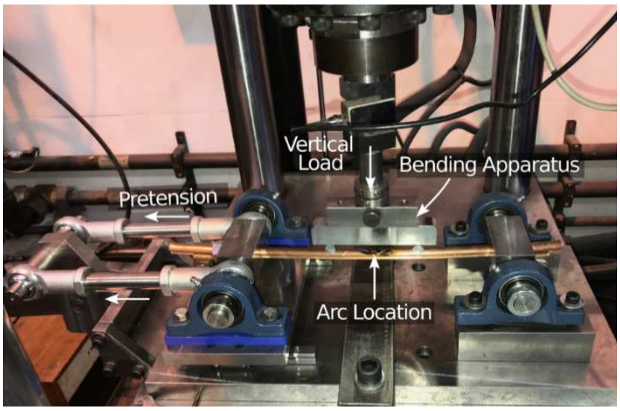

b) Arc-affected contact wire placeme

c) Tensioning weights

Figure 5 OLE fatigue apparatus

Group) installed between the actuator and four-point bending apparatus. Force data collected by the load-cell were logged to computer throughout testing. The sensitivity of the load-cell and displacement was calibrated before starting a new experiment. The experiment was automatically terminated when the loadcell detected zero vertical force due to the contact wire failure.

2.5. Fatigue Testing

Loading Conditions

The first group of samples in the fatigue testing was to set a benchmark with arc-free contact wires. In this loading condition arc-free specimens were subjected to vertical bending under axial constant tension representing the pantograph passing over the contact wire with an uplifting force (Figure *6*a).

To assess whether and how the arc damage on the surface affects fatigue behaviours of the contact wire, two sample orientations were considered in arc-affected contact wire samples. Firstly, the arc location was loaded in a conventional bending condition in which the arc location was subjected to compression stress due to the bending of the contact wire (Figure *6*b). This would represent the pantograph passing arc damage on the contact wire running surface.

The second orientation tested was selected to present a reverse bending situation which often occurs when the contact wire is connected with OLE fittings (claws, clamps or droppers) producing a change of system stiffness. The locations a few centimetres before and after of OLE fittings have been reported to be highly critical for the initiation of fatigue cracks from the bottom surface of the contact wire [3]. In this case, because the OLE fittings have high stiffness and high mass, points before and after the

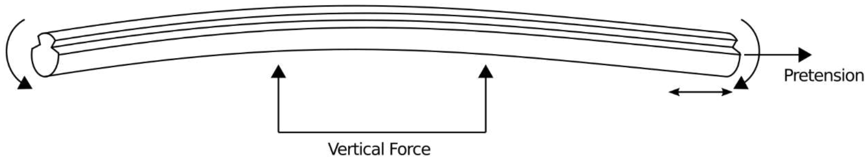

a) Arc free samples with bending

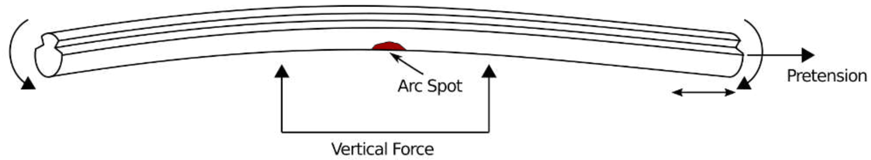

b) Arc-affected samples with bending

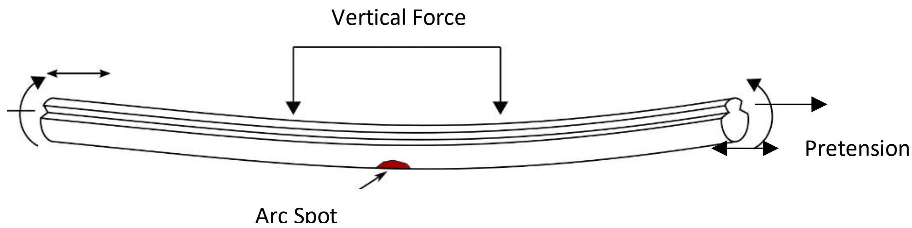

c) Arc-affected samples with reverse bending

Figure 6 Loading conditions

junction claw/OLE fittings are bent in a reverse direction, exposing the contact wire running surface to a tensile stress during the pantograph passage. Therefore, this loading condition was selected to present tension stress on the arc affected surface of the contact wire (Figure *6*c).

Appropriate Load Selection

For contact wire in a full-scale OLE span (typically 60m length) lateral load from the pantograph produces bending but also significant vertical displacement of the wire. This vertical deflection is not the primary element driving the fatigue failures but must be considered in calculating loading conditions for the test sample that are representative of the installed wire. The stress on the contact wire surface and the strain as a consequence are more appropriate parameters to associate with fatigue rather than the contact force or the vertical deflection. Regarding these factors, a strain and test force relationship was established by a finite element model in Ansys 19.1 with the contact wire under pretension. In order to mimic total displacement of the contact wire sample together with elastic and plastic deformation tensile test results data [11] including stress and strain behaviours was defined to the FE model. A tetrahedral element (type SOLID187) was used to represent the wire, with a convergence analysis was applied to the FE model to determine the optimum number of elements and ensure element quality checks were satisfied (average of aspect Ratio, Jacobian ratio and Skewness, 1.87, 0.98 and 0.24, respectively). Figure *7* shows boundary conditions and the stress distribution due to the bending of 300-mm-length of contact wire test sample.

Table 1 presents the results obtained from the FE analysis for loads exposing the contact wire to a wide range of potential service conditions for fatigue testing of OLE wire specimens under combined bending

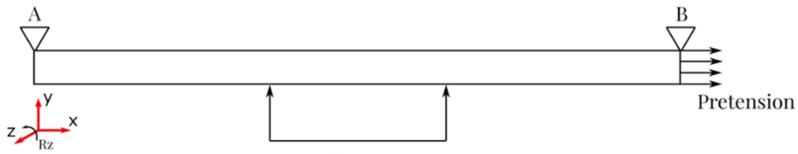

a) Load selection boundary conditions

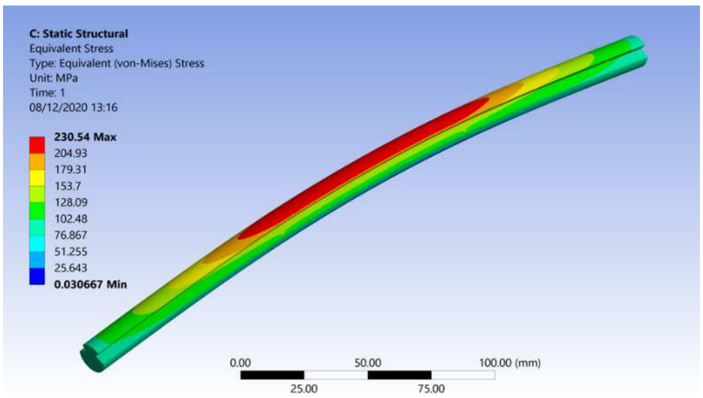

b) Stress distribution on the contact wire

Figure 7. FE model for selecting appropriate test loads, deformation exaggerated for clarity.

and tension. In the table, deflection is the vertical displacement in the centre of the contact wire relative to the end of the sample, vertical force is the selected test load for the experiments and total strain/stress corresponds to the FE analysis stress/strain results in the centre of the contact wire. Theoretical plastic strain was taken to start after strain of $3.1\text{x}10^{-3}$ which reached at 0.2% proof stress [11]. Thus, plastic deformation presented at strain values over 0.2 % proof stress. Equivalent pantograph force corresponding to the vertical test force was calculated based on an existing study concerning the relationship between contact force and maximum strain for different OLE designs.

Table 1 Load selection for fatigue testing

Deflection mm	Test Vertical Force N	Equivalent Pantograph Force in Real Scale N	Total Strain (mm/mm) 10^{-3}	Plastic Strain (mm/mm) 10^{-3}	Stress MPa
1.75	1500	221	2.020	-	229
2.05	1750	272	2.470	-	248
2.66	2000	334	3.027	-	280
3.96	2500	470	4.253	1.15	324
5.22	3000	615	5.553	2.45	347
6.25	3400	739	6.664	3.56	365

3. Results

3.1. Fatigue Life

Fatigue life results obtained from the experiments are shown in Table *2*. Data groups in the experiments were indicated with numbers from 1 to 6. In order to avoid repetition of testing conditions of arc-free bending, arc-affected bending and arc-affected reverse bending, their abbreviations, AFB, AAB and AARB were used, respectively.

Strain-life methods [20]–[22] were used to analyse and compare the fatigue life of arc-free and arc-affected contact wires, These were selected since the contact wire could be taken beyond the elastic limit, resulted in plastic deformation in some loading conditions. A regression analysis was applied to the experimental data using a second-degree exponential curve fitting method and fatigue life behaviours of the contact wire samples are presented in Figure 8. From both Table *2* and Figure 8, it can be seen that strain parameters were identical for test groups of 1,2,3 and 4 in AFB, AAB and AARB loading conditions. However, the strain parameters of Group 6 with AARB were lower than those of Group 5 with AFB and AAB. This was intentionally set to keep the fatigue life of the contact wire below cycles 10^7 so that the fatigue life curves of three loading conditions were presented in a close range without the need for extrapolation.

In Table *2*, the change in fatigue life of contact wire under arc-affected conditions (AAB and AARB) were compared relative to the AFB tests. It can be seen from results that, although the average change in fatigue life results in AAB tests relative to AFB tests were just in the vicinity of 0.3%, the AARB tests reduced the life very significantly relative to AFB by 50%.

Table 2 Cycles to the failure in the fatigue experiments of contact wire samples

		Fatigue Life (cycles)					
Test group ID	**Total Strain** 10^{-3}	**AFB** (baseline arc-free bending)	**AFB** (baseline average)	**AAB** (arc affected bending)	**AAB** (% change in life relative to baseline average)	**AARB** (arc affected, reverse bending)	**AARB** (% change in life relative to baseline average)
1	6,664	73528	72118	65785	-8.8	51366	-28.8
	6,664	70708		59698	-17.2	48642	-32.6
2	5,553	228444	219670	175654	-20.0	96028	-56.3
	5,553	210896		181546	-17.4	81311	-63.0
3	4,256	427888	439831	430582	-2.1	180193	-59.0

	4,253	410951		450653	2.5	107813	-75.5
	4,253	480655		640938	45.7	218513	-50.3
4	3,027	1650211	1453885	1321397	-9.1	720594	-50.4
	3,027	1424516		1513488	4.1	790453	-45.6
	3,027	1286928		1706759	17.4	844070	-41.9
5	2,470	7010955	6799694	7339806	7.9	-	-
	2,470	6588432		6879533	1.2	-	-
6	2,028	-	-	-	-	9665213	-
	2,028	-	-	-	-	8169431	-
	2,028	-	-	-	-	8044980	-
	2,028	-	-	-	-	7804699	-
Mean of % changes across all tests based on AFB tests					0.3		-50.3

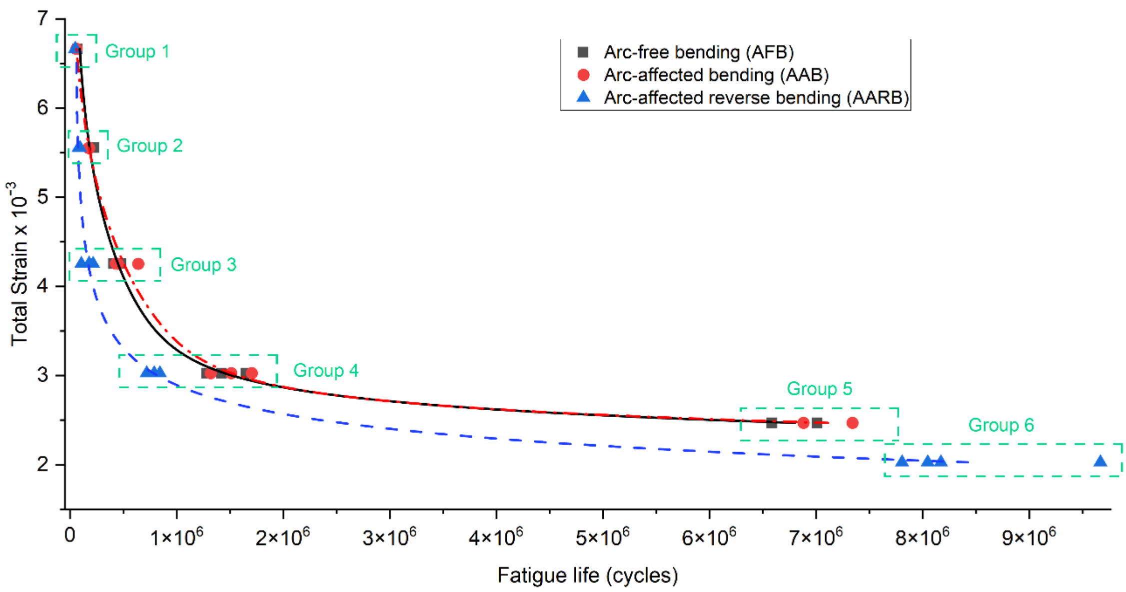

Figure 8 Exponential fitted curves of fatigue life results against total strain

What stands out in Figure 8 is that the lowest fatigue life was observed in test group 1 and they were all around 60000 cycles and very similar behaviour was seen in AFB, AAB and AARB conditions. However, in other test groups, cycles to the failure in AARB tests were different than AFB and AAB tests. The contact wire sample in AARB where the arc damage was on the tension surface of the contact wire, showed relatively shorter cycle to fatigue failure life comparing to AFB and AAB tests. The fatigue life of the samples involving arc damage on the compression surface (AAB) were very similar to fatigue life behaviours of those of arc-free, AFB.

Speaking about the difference in the fatigue life of three different experimental studies, at high strain Group 3 ($4.23x10^{-3}$), while cycles to failure in AARB was half of that in AFB, the results in AAB remained almost the same as those in AFB. However, for lower strains, Group 5 and 6, life can drop more dramatically. Considering, Group 5, the strain around $2.7x10^{-3}$, while the fatigue life of the contact wire in AFB and AAB was around $7x10^{6}$ cycles, by estimation of the fitted curve it was only in the order of $2.5x10^{6}$ cycles in AARB tests. In particular, the effect of the arc being located on the tension surface was very significant in crack initiation. All the samples in AARB tests broke from the arc location, while there were no arc-related fatigue failures in AAB tests. This indicates that arc damage in the running surface but away from OLE fittings is unlikely to degrade the contact wire fatigue life. But close to fittings (areas of ‘reverse bending’) arc damage can greatly reduce fatigue life. To better understand the main contribution of the arc damage on the surface of the contact wire to the reduction in fatigue life, a detailed fracture analysis is reported in the next section.

3.2. Fracture Analysis

Crack initiation, propagation and the failure due to the fatigue loading were seen in the detailed fracture inspection of the tested samples. Figure 9 presents the fracture surface and the crack initiation locations of the samples with three different loading condition, Group 1, Group 2 and Group 3, at high strain values (over 0.2 % proof stress) in which plastic deformation was dominant. From the results in the figure it is apparent that the crack started from the top surface of the contact wire for both cases of AFB and AAB. Since the arc damage was on the compression surface of the wire in AAB samples, the arc location did not contribute to crack initiation and did not accelerate the fatigue failure of the contact wire. Therefore, fatigue cycle results from these two cases, AFB and AAB, did not show any significant differences. On the other hand, the crack initiation in AARB case was significantly affected by the arc damage. When the samples were loaded in this configuration, arc damage on the wire’s surface was subjected to tension stress and all failures originated from the arc induced areas, propagated through the cross-section and resulted in failure (Figure *9*c). Because the crack initiation was pre-existed due to the arc damage, an accelerated fatigue failure of contact wire samples was observed. At high strain, the life of the contact wire was approximately halved since the crack initiation stage was bypassed by the pre-existed arc damage on the surface (as illustrated by the data in Table *2*). The presence of an arc site in a susceptible location (test configuration AARB) reduced fatigue life to ~50% of its value for AFB and AAB tests by effectively bypassing the natural crack initiation process. Hence, a reasonable estimate can be made that for configurations AFB and AAB, 50% of the overall fatigue life was taken up by the crack initiation process.

Additionally, fracture type and the failure of the arc affected contact wires with reverse bending under elastic strain had a distinctive crack morphology which was repeatedly produced across the tests. Figure *10* shows the contact wire fatigue failure in Group 6 with AARB condition (under elastic strain condition with reverse bending). After a crack initiated at the arc location, it propagated normal to the surface but then diverted into two directions with a large angle between them (Figure *10*c). Eventually, one of the cracks resulted in a failure, and the fatigue experiment was terminated. Measurements from the broken contact wires showed that the normal distance from crack initiation point to the start point of crack branching of the contact wire varied between 2.3 and 3 mm and the crack angle was in a range of 13 and 15 degrees relative to the longitudinal wire direction.

a) Topology of cracked area

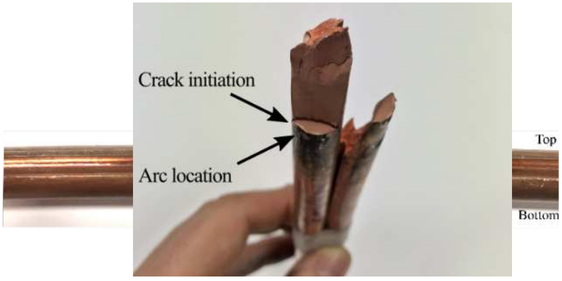

b) Cross section of the sample after failure

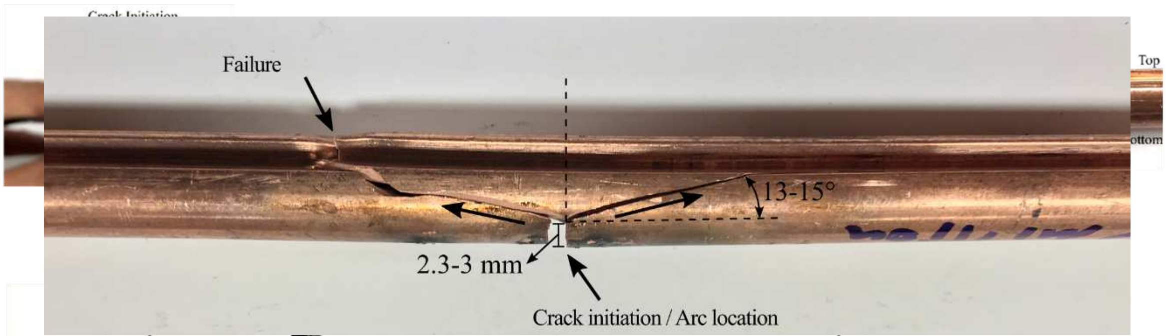

c) Crack branching directions and angles

Figure 10 Fatigue failure and crack propagation direction in Group 6 with AARB sample

Crack Initiation Arc Damage

Arc Damage

c) Arc-affected contact wire sample with reverse bending (AARB)

Figure 9 Fracture surface and crack propagation directions of tested samples at high strain

To better understand the prospective interior damage due to the arc discharge on the sample surface, the arc-induced surface itself was inspected under the microscope by sectioning through the arc location. Figure *11* presents micrographs from two control samples which were sectioned from the same wire used in baseline tests. These control samples were prepared to reveal the changes between standard contact wire, wire subject to arcing alone, and wire subject to arcing plus fatigue loading. The results were quite revealing in several ways. Firstly, the arc discharge severely affected 200 µm depth of the sample and changed grain size and shapes. Secondly, a considerable number of voids up to 100 µm diameter existed after the arc exposure. Lastly, microcracks had formed in the arc damaged area between the voids.

4. Discussions

The observed difference in fatigue life of arc-free and arc-affected wires in bending and reverse bending conditions was significant. The most prominent finding to emerge from the experiments is that all the contact wire samples in reverse bending condition (AARB) broke from the arc location while no failure originating from arc damage was observed in the conventional (AAB) bending condition. The microstructural investigation of arc-affected contact wires indicated that severe damage not only existed on the wire surface but also in the interior of the material. Particularly, voids and microcrack observed in the cross-section of the wire were the primary factors accelerating the fatigue failure and arc damage on the tension surface of the wire would behave as a pre-existed crack. The conventional crack initiation stage was bypassed by arc damage, but only when it was in a susceptible location.

It is often considered that the wear defines the service life of the contact wire; however, the fatigue problem combined with arcing can severely limit life under the reverse bending condition. The wear life of the contact wire is normally approximately 50 years. To estimate the traffic density at which a change from wear to fatigue controlled life takes place we can take the experimentally determined fatigue life for a low strain loading condition in arc-free contact wire ($7x10^6$ cycles) and assume these cycles are distributed over 50 years. In all probability wear life will limit the life of the wire to less than this, but this corresponds to 150000 pantograph passage in a year (average of ~410 passes per day) which is representative of traffic on a busy rail line [12]. However, under the reverse bending condition the fatigue life of the arc-affected contact wire was found in the order of $2.5 x10^6$ cycles which

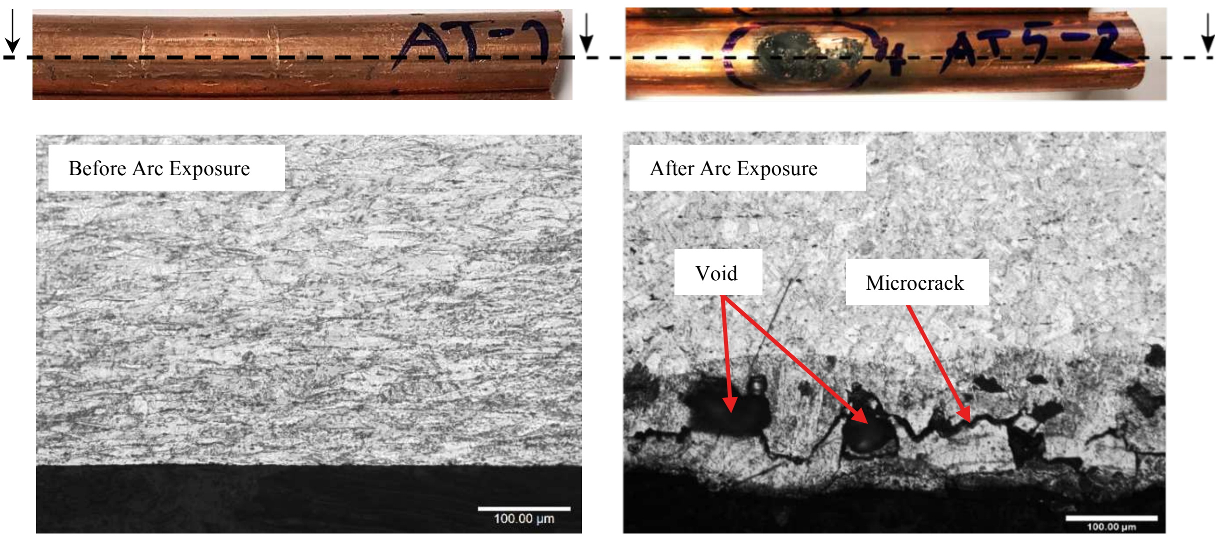

a) Arc-free control sample

b) Arc-affected control sample

Figure 11 Microstructural views of arc-free and arc-affected control samples prior to fatigue testing corresponds to just over 16 years based on the same traffic condition. So fatigue is more likely to be contact wire life limiting when it develops in locations which are subject to this bending configuration.

The arc location in the experiments was taken to be the bottom surface of the contact wire; however, these findings are also applicable to the condition in which the arc damage is elsewhere on the contact wire. Examination of wires removed from service [18] showed flashover arc damage (including sub-surface voids) over all faces of the contact wire. This may expand the number of arc events which coincide with a susceptible stress location, although development of fatigue damage would still need a high magnitude of stress (as found near joints and clamps).

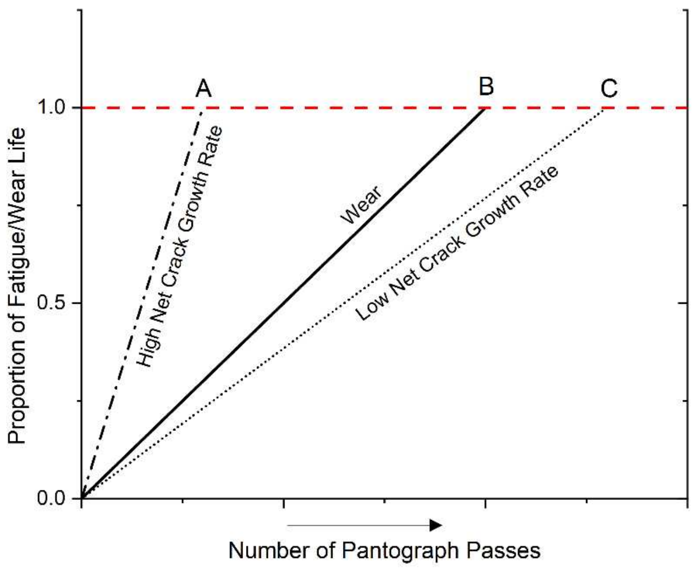

Figure *12* Theoretical fatigue and wear failure speeds of the contact wire against pantograph passes

In the current test configuration wear was absent at the bottom surface of the contact wire when considering the potential of arc damage to initiate fatigue. Arc damage may be worn away by passing pantographs as net crack growth depends on the combination of surface wear and crack tip advance. Whether the primary life limiting factor is wear or fatigue crack growth can be better explained with a diagram, Figure 12. In this figure consumption of wear or fatigue life for three scenarios (high net crack growth rate, low net crack growth rate, sliding wear) is represented against number of pantograph passes. Due to the pantograph current collection strips sliding over the contact wire surface the proportion of contact wire wear life consumed (continuous line) increases steadily, reaching the wear limit (point B, proportion of life=1) at which point reduced wire cross-sectional area means the wires should be replaced to avoid an increasing risk of failure. However, if a high net crack growth rate exists (dash-dot line) the proportion of fatigue life consumed can increase more rapidly with pantograph passes than that of wear life consumption, and the contact wire can reach fatigue failure at point A. This is prior to the wear limiting number of pantograph passes and is a fatigue dominated case. On the other hand, fatigue cracks with low net crack growth rate (dotted lines) would grow over a longer time compared to high crack growth rate and reach a life limit line at point C. In this case, the wear life reached at point B would define the contact wire life. Further research is required to understand the proportionality between wear and net crack advance shown here schematically across a range of pantograph contact loads and OLE designs.

5. Conclusions

This study sought to determine whether the surface damage generated by arcing would constitute a crack initiation point and trigger for fatigue damage in railway overhead electric lines. It was undertaken using a sequence of experimental tests in SOLARC and OLE fatigue testing apparatus. The findings indicate that arc damage on the maximum tension surface of the wire can significantly shorten the fatigue life of the contact wire. Although the fatigue life is considered longer than the wear life in the design stage, under reverse bending in combination with arcing the fatigue life of the contact wire can be shorter than the wear life. Therefore, particularly around the locations where the arcing is likely, the fatigue life of the contact wire should be taken into consideration during system design and maintenance.

These findings contribute in several ways to our understanding of how arcing can affect the service life of OLE contact wires in terms of fatigue damage. Furthermore, the fracture analysis of the arc-oriented broken samples revealed that there could be a relationship between internal voids and crack branching. Micro-cracks can occur in the contact wire material after the arc induce and this can lead branched cracks due to the fact that the straight cracks split into two by meeting micro-cracks.

Acknowledgement

Special thanks to Furrer+Frey and Network Rail for their support and collaboration, and to Dr Adam Beagles for initial direction in the investigation and helpful discussion of the work. This work was also supported by the Turkish Ministry of National Education Scholarship programme.

References

[1] BSI, "BS EN 50149: Railway applications — Fixed installations — Electric traction — Copper and copper alloy grooved contact wires," 2012. doi: 10.3403/30209002.

[2] Y. Kim, K. Lee, Y. H. Cho, Z. Guo, J. M. Koo, and C. S. Seok, "Fatigue safety evaluation of newly developed contact wire for eco-friendly high speed electric railway system considering wear," *International Journal of Precision Engineering and Manufacturing - Green Technology*, vol. 3, no. 4, pp. 353–358, Oct. 2016, doi: 10.1007/s40684-016-0044-0.

[3] J. P. Bianchi, E. Balmes, and M.-L. Nguyen-Tajan, "Dynamic stress prediction in catenary wires for fatigue analysis," *The Dynamics of Vehicles on Roads and Tracks - Proceedings of the 24th Symposium of the International Association for Vehicle System Dynamics, IAVSD 2015*, no. October, 2016, doi: 10.1201/b21185-160.

[4] P. Hu, J. Liang, and W. Fan, "Dynamic fatigue reliability of contact wires based on dynamic simulation of high-speed pantograph-catenary," vol. 020152, no. May, p. 020152, 2017, doi: 10.1063/1.4982517.

[5] A. Beagles, D. Fletcher, M. Peffers, P. Mak, and C. Lowe, "Validation of a new model for railway overhead line dynamics," *Proceedings of the Institution of Civil Engineers - Transport*, vol. 169, no. 5, pp. 339–349, Oct. 2016, doi: 10.1680/jtran.16.00020.

[6] Y. Kim *et al.*, "Fatigue life prediction method for contact wire using maximum local stress," *Journal of Mechanical Science and Technology*, vol. 29, no. 1, pp. 67–70, Jan. 2015, doi: 10.1007/s12206-014-1210-3.

[7] C. Yamashita and A. Sugahara, “Influence of Mean Stress on Contact Wire Fatigue,” *Quarterly Report of RTRI*, vol. 47, no. 1, pp. 46–51, 2006, doi: 10.2219/rtriqr.47.46.

[8] International Electrotechnical Commission and International Electrotechnical Commission. Technical Committee 7, *Overhead lines : methods for fatigue testing of conductors*.

[9] A. Sugahara, C. Yamashita, and T. Usuki, “Applicability of Rain Flow Method to Fatigue Life Span Estimation of Overhead Contact Wire,” *Quarterly Report of RTRI*, vol. 51, no. 4, pp. 176–181, 2010, doi: 10.2219/rtriqr.51.176.

[10] G. Zhen *et al.*, “Bending fatigue life evaluation of Cu-Mg alloy contact wire,” *International Journal of Precision Engineering and Manufacturing*, vol. 15, no. 7, pp. 1331–1335, 2014, doi: 10.1007/s12541-014-0473-z.

[11] O. Sunar, “Arc Damage Identification and Its Effects on Fatigue Life of Contact Wires in Railway Overhead Lines (PhD Thesis),” 2021. [Online]. Available: http://etheses.whiterose.ac.uk/28205/

[12] Nguyen-Tajan *et al.*, “Fatigue crack initiation risk analysis and crack propagation modelling in the catenary contact wire of high speed lines,” in *World Congress on Railway Research (WCRR)*, 2013, pp. 1–7.

[13] R. Stainton, “Network Rail Safety Bulletin Arthur Flury Single Rod Neutral Section Installations – Risk of uncontrolled release of Contact Wire tension, Technical Report IGS 301,” London, 2013.

[14] V. N. Li and S. v. Klimenko, “Determination of thermal softening of overhead wire exposed to an electric arc effect,” *Russian Electrical Engineering*, vol. 87, no. 2, pp. 77–79, Feb. 2016, doi: 10.3103/S1068371216020115.

[15] S. Klimenko and V. Li, “Methodology for Assessing the Condition of the Contact Wire by the Value of Thermal Softening,” in *Advances in Intelligent Systems and Computing*, 2020, vol. 1115 AISC, pp. 138–145. doi: 10.1007/978-3-030-37916-2_15.

[16] J. P. Massat, T. M. L. Nguyen-Tajan, H. Maitournam, E. Balmès, A. Bobillot, and J.-P. Massat, “Fatigue analysis of catenary contact wires for high speed trains,” 2011.

[17] O. Sunar, D. Fletcher, and A. Beagles, “Laboratory Assessment of ARC Damage in Railway Overhead Contact Lines With a Case Study on Copper-Silver and Low Oxygen Content Copper,” *IEEE Transactions on Power Delivery*, vol. 36, no. 5, pp. 3074–3081, Oct. 2021, doi: 10.1109/TPWRD.2020.3032798.

[18] Ö. Sunar and D. Fletcher, “Case study: Mechanical and metallurgical investigation of arc damage in overhead line contact wires,” *The Journal of Permanent Way Institution*, vol. 139, no. 3, pp. 34–39, 2021.

[19] “ASTM D6272-10, Standard Test Method for Flexural Properties of Unreinforced and Reinforced Plastics and Electrical Insulating Materials by Four-Point Bending, ASTM International,” 2017.

[20] F. C. Campbell, *Fatigue and Fracture: Understanding the Basics*, vol. 53, no. 9. 2012.

[21] S. S. Manson, *Behavior of materials under conditions of thermal stress*, vol. 2933. National Advisory Committee for Aeronautics, 1953.

[22] L. F. Coffin, “The Problem of Thermal Stress Fatigue in Austenitic Steels at Elevated Temperatures,” *Symposium on Effect of Cyclic Heating and Stressing on Metals at Elevated Temperatures*, pp. 31-31–22, 1954, doi: 10.1520/stp48000s.